Available online at www.sciencedirect.com
ScienceDirect
Journal of Solid State Chemistry 180 (2007) 3188–3195
JOURNAL OF SOLID STATE CHEMISTRY
www.elsevier.com/locate/jssc

Hydrothermal synthesis, characterization and its photoactivity of CdS/Rectorite nanocomposites

Jiangrong Xiao[a], Tianyou Peng[a,b,*], Ke Dai[a], Ling Zan[a], Zhenghe Peng[a]

[a]*Department of Chemistry, Centre of Nanoscience and Nanotechnology Research, Wuhan University, Wuhan 430072, China*
[b]*Hubei Key Laboratory for Catalysis and Material Science, College of Chemistry and Material Science, South-Central University for Nationalities, Wuhan 430074, China*

Received 26 May 2007; received in revised form 5 August 2007; accepted 6 September 2007
Available online 14 September 2007

Abstract

CdS/Rectorite nanocomposites were prepared through hydrothermal method by using $Cd[NH_2CSNH_2]_2Ac_2$ complex as precursor of CdS which was derived from cadmium acetate and thiourea. The obtained nanocomposites were characterized by X-ray diffraction (XRD), Fourier transfer infrared spectra (FTIR), diffusion reflection spectra (DRS), transmission electron microscopy (TEM) and the selected area electron diffraction (SAED) patterns. Experimental results indicate that CdS exist in at least three forms: CdS adsorbed at surface, CdS pillared in montmorillonite-like layers of Rectorite and CdS pillared in the new layered structure formed during the hydrothermal process. Those CdS crystals are hexagonal symmetry. The photoactivity and photostability of the obtained CdS/Rectorite nanocomposites are improved significantly compared to that of the reference Rectorite and pure CdS.

Keywords: CdS; Pillared; Nanocomposite; Rectorite; Photocatalytic activity

1. Introduction

Numerous researches have been focused on the pillared clays in the past decades due to its extensive applications in absorber and catalyst [1–4]. In general, the pillared clays were prepared through ion exchange reaction between the clay and polyoxocations containing Al, Zr or Ti, etc., which can exchange with the exchangeable cations in the interlayer of clays [5–11], and the resulting pillared interlayer clays were previously described as a new kind of microporous materials [12,13]. Rectorite is a regular clay mineral, and there are rich sources in Hubei, China. It is an interstratified layered silicate mineral consisting of a regular (1:1) stacking of mica-like layers and montmorillonite-like layers [14]. A schematic representation of the Rectorite structure [15] is given in Fig. 1. The cations of Na^+, K^+, Mg^{2+} and Ca^{2+} lie in the interlayer regions of 2:1 mica-like layers and 2:1 montmorillonite-like layers, but the exchangeable hydrated cations only distribute in the montmorillonite-like interlayers, which can be exchanged by monovalent and divalent cations through charge compensation [14]. Pillared Rectorites have been prepared through a cation exchange followed by calcination process at an elevated temperature [11,16–20]. For example, the pillaring reactions were performed with an excess of aluminum chlorhydrate (ACH) solutions, and the reaction products were collected by centrifugation and extensively washed with distilled water. Subsequently, the washed samples were air-dried at room temperature and then oven-dried at 100 °C for an additional 4 h to obtained the Al_{13}-pillars Rectorites [15].

As a semiconducting material, besides its interesting optical properties [21,22], CdS is also interesting for the special photocatalytic activity and it is active under visible light for hydrogen production from photosplitting water [23]. CdS is not stable in aqueous solutions under irradiation due to the electrochemical corrosion, but it has been reported that the supported CdS has a performance

*Corresponding author. Department of Chemistry, Centre of Nanoscience and Nanotechnology Research, Wuhan University, Wuhan 430072, China. Fax: +86 27 6875 4067.
E-mail addresses: typeng@whu.edu.cn (T. Peng), pengzh@chem.whu.edu.cn (Z. Peng).

0022-4596/$ - see front matter © 2007 Elsevier Inc. All rights reserved.
doi:10.1016/j.jssc.2007.09.009

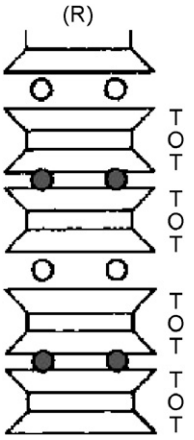

Fig. 1. Schematic representation of Rectorite structure [15]. The T–O–T three layers sequence is represented by trapezoid and rectangles. T is tetrahedral and O is octahedral sheet. Exchangeable and non-exchangeable charge compensating cations are represented by open and solid circles, respectively.

and stability superior to that of the unsupported one, because the active ingredient is dispersed on the supports, and the supports provide heterojunctions for electrons and holes that restrict the charge recombination and S^{2-}-oxidation [24–26]. For example, CdS has been intercalated into the interlayers of semiconducting layered compounds to form $CdS/H_2Ti_4O_9$, $CdS/K_2Ti_4O_9$, and $CdS/H_4Nb_6O_{17}$ compositions [24–26]. Shangguan and Yoshida [25] have reported that the photoactivities of $CdS/K_2Ti_4O_9$, $CdS/K_2Ti_{3.9}Nb_{0.1}O_9$ are superior to those of pure CdS and the physical mixture of CdS and relative metal oxides. Furthermore, pillared natural calys have already been researched extensively [27–33]. Some semiconductors (e.g. CdS, TiO_2) pillared natural calys, especially montmorillonite, have also exhibited promising applications as photocatalysts for the degradation of contaminations and hydrogen production from photosplitting water.

Although the pillared Rectorites as catalysts have been studied extensively [29,30], those researches mainly concentrated on the oil gas decompositions. Up till now, Rectorite has seldom been applied in the photodegradation of organic contaminations as photocatalysts. Very recently, CdS/Rectorite nanocomposites were synthesized via cation-exchange reaction followed by sulfurization process in our group [34]. The photocactivity and photostability of the pillared nanocomposites were enhanced significantly comparing with the bare Rectorite and pure CdS. However, some other preparation pathways for CdS/Rectorite nanocomposites remain absolutely necessary because: (1) the above two-step processes need hazardous H_2S gas, and are burdensome and time-consuming [34]; (2) the loading amount of CdS in nanocomposite is limited and uncertain due to the washing, the lower driving forces and the thermodynamics factors during ion exchange process; (3) the very limited expansion in *d*-spacing (ca. 0.07 nm) means that the pillars (CdS) among the interlayers of Rectorite is very small in particle size and loading amount. All those factors might retard the further improvement in the visible light absorption of CdS and photoactivity of the composites. Hydrothermal method has been applied for the syntheses of CdS/montmorillonite [27] and TiO_2/montmorillonite [28] composites, in which a relatively larger amount of CdS and TiO_2 existed in the pillared forms and nanoparticles. To the best of our knowledge, however, there is still no other literature focused on the hydrothermal synthesis of the CdS/Rectorite nanocomposites and its photocatalytic performances. Herein, CdS/Rectorite nanocomposites were synthesized via a hydrothermal process. Compared with the two-step processes described in our previous publication [34], hydrothermal process is a more effectual, simpler and safer method for the fabrication of CdS/Rectorite, at least, it can provide more CdS loading amount without the uncertain loss of CdS during the synthesis processes. It will be beneficial for improving the visible light absorption of the composites. Moreover, ICP-AES technology was also applied to measure Cd concentration in the suspensions after photodegradation experiments to ravel the detailed photostability of the resulting composites.

2. Experimental section

2.1. Materials

Rectorite clay was supplied by Hubei Celebrities Rectorite Technology Co., China. The composition of Rectorite are listed in Table 1 (GBW(E)070063). As can be seen, impurities such as, TiO_2 and Fe_2O_3, coexisted in this Rectorite clay. And the cation exchange capacity (CEC) is 44.91 meq/100 g Rectorite, the average particle size is 0.82 μm. The *d*-spacing (d_{001}) is 2.46 nm, which is contribution from the mica-like layer (*d*-spacing is ca. 0.96 nm) and the montmorillonite-like layer (*d*-spacing is ca. 1.50 nm). And it is composed by the structural formula of the mica-like $(Na_{0.79}K_{0.39}Ca_{0.26})_{1.44}Al_4(Si_6Al_2)_8O_{22}$ and montmorillonite-like $(Ca_{0.55}Na_{0.02}K_{0.01}Mg_{0.03})_{0.61}(Al_{4.1}Fe_{0.09}Mg_{0.07})_{4.26}(Si_{6.46}Al_{1.54})_8O_{22}$. The cadmium acetate ($CdAc_2 \cdot 2H_2O$, AR) was supplied by Sinopharm Chemical Reagent Co., China, thiourea ($CS(NH_2)_2$, AR) was supplied by Tianjin Hengxin Chemical Reagent Co., China, Rhodamine B (RB) (AR) was supplied by the Third Shanghai Reagents Co., China. All reagents were used without further purification.

2.2. Preparation of CdS/Rectorite nanocomposites

CdS/Rectorite nanocomposites are prepared as follows: 2.0 g of Rectorite was dispersed into 50 ml of distilled water by stirring vigorously for 2 h to obtain 4.0 wt% Rectorite suspensions. The $CdAc_2 \cdot 2H_2O$ and $CS(NH_2)_2$ (molar ratio is 1:2) were dissolved into 15 ml of distilled water, and followed by ultrasonic treatment for 5 min. Accordingly, the metal–thiourea complex $Cd[NH_2CSNH_2]_2Ac_2$, the precursor of CdS was produced, which can be described

Table 1
The compositions of the rectorite (GBW(E)070063)

Component	SiO_2	Al_2O_3	Fe_2O_3	CaO	MgO	TiO_2	K_2O	Na_2O	MnO	P_2O_5	F
Mass (%)	44.31	35.60	1.50	4.05	0.35	2.46	1.12	1.24	0.01	0.41	0.08

as following reaction:

$$CdAc_2 + 2CS(NH_2)_2 = Cd[NH_2CSNH_2]_2Ac_2.$$

Subsequently, the precursor was added dropwise to above Rectorite suspensions under continuously stirring. And then this obtained aqueous suspension was poured into a set of Teflon hydrothermal containers and then hydrothermally treated at 160 °C for 8 h. After cooled to room temperature, the samples were washed with distilled water and ethanol, respectively. And then, the samples were desiccated at 60 °C. The adding concentrations of $CdAc_2 \cdot 2H_2O$ were 0, 1.0, 2.0, 3.0 and 4.0 mmol/4 g Rectorite, respectively. And the obtained samples are denoted as CR0, CR1, CR2, CR3, and CR4. For example, the CR3 means that the concentration of $CdAc_2 \cdot 2H_2O$ is 3.0 mmol/4 g Rectorite. The pure CdS is obtained under identical experimental conditions, and the CR0 is the reference Rectorite.

2.3. Characterization of materials

The XRD patterns of the prepared products were recorded by using a XRD-6000 powder diffractometer (Shimadzu, Japan) with Cu$K\alpha$ as a radiation. FT-IR spectra on pellets of the samples with KBr were recorded on a Fourier transfer infrared spectra (FTIR)-8201PC spectrometer (Nicolet, America). Transmission electron microscopy images and the selected area electron diffraction (SAED) patterns were obtained on a LaB6 JEM-2010 electron microscope (Japan Electronics, Japan). UV–Vis diffuse reflectance spectra (DRS) were performed with a Cary 5000 UV–Vis-NIR spectrophotometer equipped with an integrating sphere (Varian, America).

2.4. Photocatalytic activity and photostability tests

The photocatalytic degradation of RB was measured at ambient pressure and room temperature in a set of home-made photochemical reaction equipment. The light source was a 250 W Hg lamp, and a surrounding water jacket (Pyrex) to cool the lamp was displaced around the lamp. The distance between the samples and the lamp was 10.0 cm. Thirty milligrams of photocatalysts were added into 50 ml RB aqueous solution with consistence of 5.0 mg/l. The suspensions were stirred continuously for 45 min to aim at the adsorption equilibrium of RB onto the surfaces of CdS/Rectorite nanocomposites in the dark before irradiation. And then the suspensions were irradiated for 90 min under magnetically stirring. The photocatalysts were removed by centrifugation, and the supernatant liquid was examined using a Shimadzu UV-240 spectrophotometer. For comparison, CR0 and the pure CdS were also been conducted under an identical experimental condition. For evaluating the photostability of the products, the photodegradation experiments of the same photocatalyst had been repeated for five times under an identical experimental condition too.

3. Results and discussion

3.1. X-ray diffraction (XRD) analysis

The low-angle XRD patterns of the original Rectorite and CR0 are depicted in Fig. 2A. Simultaneously, the low-angle XRD patterns of CdS/Rectorite nanocomposites at different concentration level are shown in Fig. 2B. As can be seen from Fig. 2A, the d_{001} diffraction peak at $2\theta = 3.64^\circ$ for the original one is corresponding to the d-spacing of 2.43 nm, which is similar with the reference value as described in experimental section. Whereas, the d_{001} diffraction peak for CR0 shifts from to $2\theta = 3.36^\circ$ combined with greatly decrease and broadening in the peak intensity as well as appearances of a new broad diffraction peaks centered at 2.44°. It can be ascribed that Rectorite silicate layered structures were partly destroyed, exfoliated and/or reconstructed to new layered structures with larger intergallery spaces during the hydrothermal processes. Furthermore, the diffraction peaks at $2\theta = 6.12^\circ$, 7.08°, 8.84° and 9.70° for the original one also shifts to lower angle regions with different extent. Especially, the diffraction peak at 9.70°, which can be assigned to the d_{001} peak of the mica-like layers in Rectorire, shifts to lower angle region (9.47°). Those shifts in diffraction peaks might imply that not only montmorillonite-like layers but also the mica-like layers in Rectorite have been hydrated during the hydrothermal process, and which can result in the d-spacing expansion of intergallery spaces. This is obvious different from the observation on our previous CdS/Rectorite nanocomposites derived from two-step processes [34], in which just very limited d-spacing expansions (ca. 0.07 nm) occurred and there is no any new diffraction peak appeared during the cation-exchange and sulfurization processes. Namely, the previous two-step process can just exchange the hydrate cations in the montmorillonite-like layers, but the regular (1:1) stacking structures of the interstratified layered silicate mineral as well as the mica-like layers cannot be markedly affected. Whereas the regular stacking microstructures of Rectorite have been partly destroyed, exfoliated and/or reconstructed during the present hydrothermal process. The advantages and

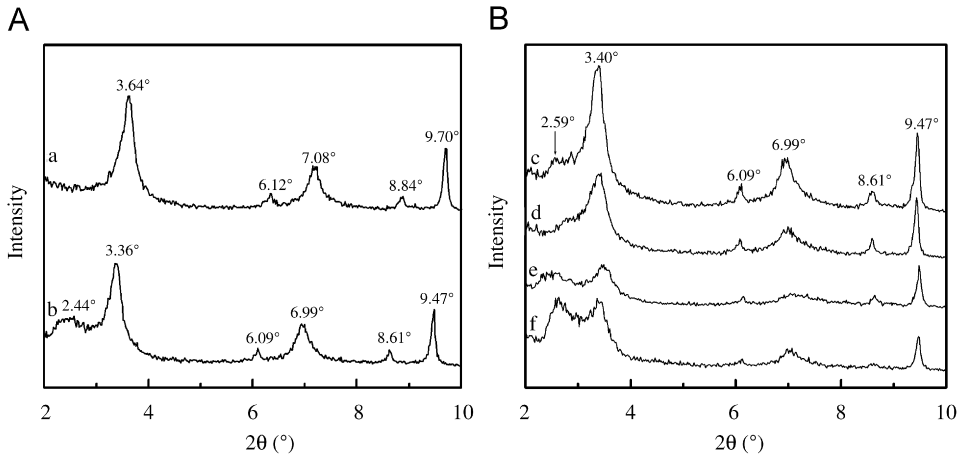

Fig. 2. (A) Low-angle XRD patterns of the obtained samples: (a) the original Rectorite, (b) CR0, (c) CR1, (d) CR2, (e) CR3 and (f) CR4.

disadvantages of this change in microstructures on the photoactivity of the resulting composites will be evaluated in the following section.

As can be seen from Fig. 2B, the d_{001} diffraction peaks was shifted to $2\theta = 3.40^\circ$ compared with the original Rectorite ($2\theta = 3.64^\circ$), which can be ascribed to CdS insertion into the intergallery spaces of montmorillonite-like layers in Rectorite [27,28]. And all above diffraction peaks for the original Rectorite also can be observed obviously for the CdS/Recrotite. The positions of those diffraction peaks are basically unchangeable compared with the reference one (CR0) except for the formation of a new broad peak centered at 2.59° concomitant disappearance of 2.44°. Upon increasing $Cd[NH_2CSNH_2]_2Ac_2$ addition amount, the d_{001} diffraction peaks became decrease and broadening in intensity, implying that the ordered layer structure of Rectorite destroyed gradually, e.g. some layered structures in Rectorite have exfoliated. The new broad peak at about $2\theta = 2.44^\circ$ for CR0 disappeared after addition of CdS in the sample combined with the appearance of a new broad centered at $2\theta = 2.59^\circ$ for CR1. This new broad diffraction peak changes gradually with different extent shifts upon increasing the addition amount of $Cd[NH_2CSNH_2]_2Ac_2$. It might be attributed that those exfoliated mica and montmorillonite structures can further reconstruct and/or form new layered structures, and in which the CdS derived from the $Cd[NH_2CSNH_2]_2Ac_2$ is inserted. Therefore, it is rational to conclude that the CdS existed in at least three forms: CdS adsorbed at surface, CdS pillared in montmorillonite-like layers of Rectorite and CdS pillared in the new layered structure formed during the hydrothermal process, though the latter is very limited as observation from Fig. 2B. This observation is also obvious different from the observation on our previous CdS/Rectorite [34], in which very limited *d*-spacing expansions occurred and CdS pillars with very small size formed. Whereas, the shift in d_{001} diffraction peaks (from $2\theta = 3.64^\circ$ to 3.40°) concomitant formation of new diffraction peak is much larger than that (from 3.65 to 3.85) in previous publication, implying that there are more CdS pillars and/or nanoparticles with much larger size in the nanocomposites. The formation mechanism for the new layered structures during the present conditions is under progress.

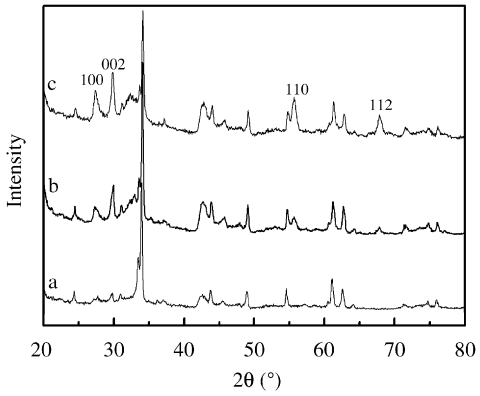

Fig. 3. High-angle XRD patterns of the obtained samples: (a) CR0, (b) CR1 and (c) CR4.

The high-angle XRD patterns of CR0, CR1 and CR4 are shown in Fig. 3. As evidenced from Fig. 3b and c, the diffraction traces at $2\theta = 24.9^\circ$, 26.5°, 28.3°, 43.8°, and 51.9° can be ascribed to d_{100}, d_{002}, d_{101}, d_{110} and d_{112} diffraction peaks of the hexagonal CdS crystal phase (JCPDS 41-1049, $P6_3mc$; $a = 0.41409$ nm, $c = 0.67198$ nm), and those diffraction peaks become more apparent as increasing addition amount of $Cd[NH_2CSNH_2]_2Ac_2$. The stronger and sharper diffraction peaks of CdS suggest that more CdS crystallites are produced when the addition amount of $Cd[NH_2CSNH_2]_2Ac_2$ is increased [22,24,27]. This increase is logical simply because more precursor feed will be more favorable to the production and crystal growth of CdS during the hydrothermal processes. Although the pillared particle sizes are still very small, the diffraction traces ascribed to the hexagonal CdS (e.g. CR4) are much higher and obvious than that in our

previous products though CR4 (e.g. 4.0 mmol CdS/4 g Rectorite) has 4 times lower nominal composite amounts than the corresponding previous composites (e.g. 4.0 mmol/g CdS/Rectorite) [34]. Simultaneously, the stronger and sharper diffraction peaks must be due to more CdS existed in the outer layer and/or the interlayers of the new formed layered structures as described above, since the very small nanoparticles intercalated in the montmorillonite-like layers are not enough to show so obvious diffraction traces. All those results indicate that the present hydrothermal processes lead to formation of CdS nanoparticles with higher loading amount, larger particle size, more perfect crystal as well as obvious changes in microstructures of the Rectorite compared with our previous method [34].

3.2. Microstructure analysis

Fig. 4 shows the transmission electron microscopy (TEM) photographs of CR4 composite material. The sheet-like morphologies can be clearly observed, which is the characteristic of exfoliated flakes for the layered structures (like Rectorite) during the TEM observation. As can be seen from Fig. 4B, some conglomeration of CdS nanoparticles lie on the outer surfaces of sheet-like structures as shown in the rectangle regions. However, there are less CdS nanoparticles adsorbed on the outer surfaces of our previous nanocomposites [34].

The SAED pattern was conducted in the region of the white circle as shown in Fig. 4B, there exist some obvious nanoparticles in the selected region. This SAED pattern displays a symmetric array of sharp diffraction spots for hexagonal CdS (JCPDS 41-1049), indicating that CdS exists as single crystal. Whereas for the selected region in Fig. 4A without any obvious nanoparticle, the SAED pattern shows that the diffraction rings of polycrystalline phase combined with sharp diffraction spots. In other word, the diffraction dots for the crystallized CdS are distinguishable from the diffraction rings of the polycrystalline clay, which is also consistent with the wurtzite CdS crystal (JCPDS 41-1049) of hexagonal symmetry. These experimental facts indicate that the surrounding of the CdS crystalline is polycrystalline Rectorite with low crystallinity. Namely, CdS nanocrystallites have inserted into the intercalary spaces of Rectoitre to form CdS pillared nanocomposite materials. Based on all above discussion, we can conclude that the formed CdS crystallites lie in the interlayers as pillars and the nanoparticles adsorbed on the outer surfaces of Rectorite, which is consistent with above conjecture on CdS existing in three forms in the resulting composites. Whereas there was seldom CdS particles are observed on the surfaces of the previous composites (refer to Fig. 5b in [34]) due to the effective removal of the surface-absorbed Cd^{2+} during the washing procedure. Therefore, the coexisting amount of CdS in the present nanocomposites is much higher than that in the previous one, which might be beneficial for making the best of the optical property of CdS.

3.3. FT-IR spectra

Fig. 5 shows the FTIR spectra of CR0, CR1, CR2 and CR4. As can be seen, there are five pairs of peaks at ca. 480/543, 713/750, 913/948, 1021/1054, 1085/1121 cm^{-1} in all of the samples, which are the characteristic peaks contributed from the Rectorite [6,35,36]. Peaks located at the intermediate frequency regions are changeless and the intensities of these peaks are decreased slightly upon increasing the nominal amount of $Cd[NH_2CSNH_2]_2Ac_2$ precursor, implying that the silicate layer main structures of the Rectorite are remained mostly in the present prepared process, which is similar with the results of the Ti-pillared Rectorite [37]. It is believed from Fig. 5 that the broad peaks at ca. 3636, 3400 and 1634 cm^{-1} are attributed to the surface-adsorbed water and the hydroxyl groups [35]. The intensities of broad peaks at around 3400 cm^{-1},

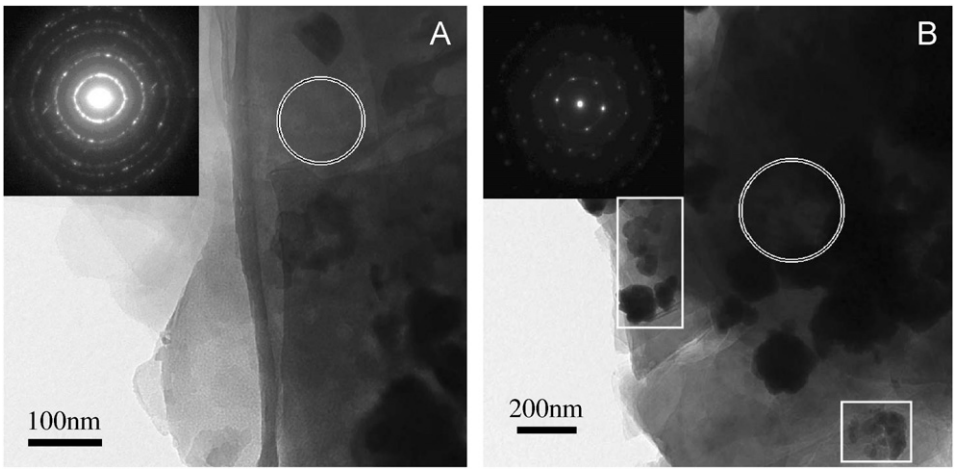

Fig. 4. TEM images and the selected area electron diffraction patterns of CR4: (A) field of sight without adsorbed CdS particles; and (B) field of sight with adsorbed CdS particles.

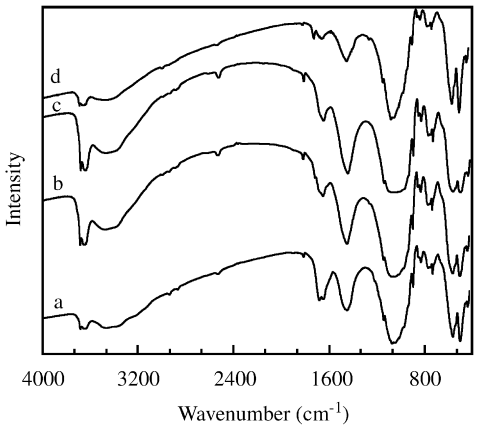

Fig. 5. FTIR spectra of the obtained samples: (a) CR0, (b) CR1, (c) CR2, and (d) CR4.

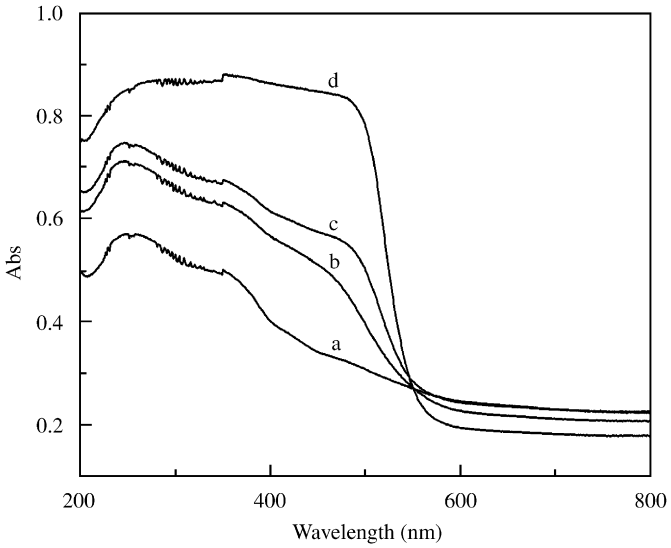

Fig. 6. UV–Vis diffuse reflectance spectra (DRS) of the obtained samples: (a) CR0; (b) the physical mixture of 1.0 mmol CdS and 1.0 g Rectorite; (c) CR1; and (d) CR4.

ascribed to the surface-adsorbed water in the FTIR patterns of the CdS/Rectorite decrease as the nominal amount of CdS per Rectorite increasing, suggesting that CdS pillars partly deplete the adsorbed water in the regions of Rectorite. Compared with the reference Rectorite, the intensity of peaks arising from the hydroxide (OH) deformations (e.g., ca. 874 and 916 cm^{-1}) linked to Al and/or Mg ions are lower for the CdS/Rectorite nanocomposites. Breakup of the 1:1 interstratified regular stacking structure of double octahedron montmorillonite-like crystallite at 2:1 ratio and mica-like crystallite at 2:1 ratio for the Rectorite may affect the position or environment (e.g., nearest neighbor atoms) of these metal ions, thus reducing the intensity of the structural OH groups linked to them. Moreover, it is also expected to result in an increase in terminal OH groups. This can be observed by the relative increase in the intensity of the OH peak at ca. 3636 cm^{-1} in Fig. 5 for the CdS/Rectorite nanocomposites. Those observations indicate that the montmorillonite-like crystallite and mica-like structure of the Rectorite remained almost unchanged and the changes might mainly occurred in the stacking structure of the Rectorite to form new layered structures as described in above sections.

3.4. UV–Vis diffuse reflectance spectra

The UV–Vis diffuse reflectance absorbance spectra (DRS) for CR0, CR1 and CR4 are shown in Fig. 6. As can be seen, the reference Rectorite shows visible light absorption ability. It is rational that the sample contains some impurities such as ferric oxide and titania as indication in Table 1. The composites show obviously red shifts compared with the CR0, and these red shifts enhances gradually upon increasing the addition amount of CdS precursor. It is declared that the larger CdS particle sizes are generated in the composites, which is consistent with the observation from XRD patterns (Fig. 3) and the previous results [22,24,26]. The CdS/montmorillonite [22,24] and CdS/laponite clay [26] nanocomposites also show that red-shift on the absorption onset enhanced with increasing the concentration of CdS. Furthermore, the band gap energy of CdS/Rectorite composites is larger than that of the physical mixture of Rectorite and CdS as shown in Fig. 6b. This difference can be attributed to the smaller particle sizes of CdS in the CdS/Rectorite composites compared with the pure CdS. Namely, the incorporation of CdS nanoparticles into the intergallery spaces of the Rectorite could suppress the particle growth, and this, in turn, resulted in the quantum size effect, consequently, the band gap energy enlarging [38].

Although the nanocomposites show obviously blue shifts in the onset light absorption compared with the pure CdS derived from the same hydrothermal process, the absorbance of the product significantly enhance in range of 200–580 nm upon increasing the additional amount of $Cd[NH_2CSNH_2]_2Ac_2$. For example, CR4 shows an almost similar DRS spectrum with the pure CdS. It is notably higher than that in the DRS of our previous products though CR4 (e.g. 4.0 mmol CdS/4 g Rectorite) was derived from 4 times lower nominal composite amounts than that of our previous nanocomposites (e.g. 4.0 mmol/g CdS/Rectorite) (refer to Fig. 8 in [34]). This difference in light absorption can be attributed to the differences in the real loading amount and the existing forms of CdS between the two kinds of composites. On one hand, much larger loading amount of CdS exists in the present nanocomposites as described above. On the other hand, much more CdS adsorbs on the surfaces of materials than our previous one [34]. Obviously, the present nanocomposites with the more CdS loading show much better visible light absorption property than that of our previous one derived from ion-exchange reaction [34], which is beneficial for the improvement of the photoactivity of the resulting materials.

3.5. Photoactivity tests

Blank experiments conducted in the photoreactor without nanocomposite showed less than 0.5% RB was decomposed after 90 min UV irradiation, indicating that RB has a good photostability under the UV light irradiation. The relationship between the photodegradation efficiency of RB and the irradiation time are depicted in Fig. 7. For comparison, it also gives the photocatalytic experiment results of CR0, and the pure CdS (3.8 mg) according to 30 mg 4.0 mmol/4 g CdS/Rectorite, respectively. For CR4, 87% RB was photodegraded after 90 min irradiation, whereas just 57% and 15% RB were photodegraded for CR0 and the pure CdS, respectively. Moreover, CR2 with lower CdS loading showed an almost same photodegradation efficiency of RB as that of CR4 during the 90 min UV irradiation. The comparable efficiency suggest that the loading amount of CdS in Rectorite might have an optimal value for the photodegradation of RB, which should be further investigated.

For effective degradation, the organic materials should be preconcentrated on photocatalysts' surfaces to effectively trap the respective reactive radicals and/or photogenerated carriers. In other word, the adsorptive property of photocatalysts is very important to determine the photoactivity. The surface adsorptive properties of the original Rectorite, CR0, CR1, CR2, CR3, CR4 and CR5 are 0.56, 0.92, 1.08, 1.10, 1.35, 1.46 and 1.35 mg/g, respectively. As can be seen, the hydrothermal treatment can effectively enhance the surface absorptive property of Rectorite itself. It can be ascribed to the changes in the microstructures of Rectorite as observed above. And the adsorptive amount also increase upon enhancing the CdS loading amount from 1.0 to 4.0 mmol CdS/4 g Rectorite, whereas it will decrease with enhancing the CdS loading amount to 5.0 mmol CdS/4 g Rectorite. It can be due to the too much CdS adsorbed on the surfaces of composites and retard the further adsorption of RB. Furthermore, as it is expected, the photoactivities of nanocomposites also show a similar change trends with the absorptive properties. Those results indicate that the photoactivities of CR4 and CR2 were enhanced significantly comparing with CR0 and the pure CdS. It is attributed to the better absorptive property and more quickly electron transfer through the interlayers into the surfaces of the host layers, which is beneficial for retarding the recombination of the photogenerated carriers, and consequently, improving the photoactivity [25]. On the other hand, the relatively small CdS particle size is beneficial for the higher photogenerated voltage, more effective electron–hole separation due to the quantum effect. Furthermore, the layer structure is also beneficial for the transfer of the object (RB) and the photodegradation products. Therefore, the improved photoactivity of CdS/Rectorite nanocomposite can be attributed to the surface adsorptive property, the cooperation or synergetic action of the CdS and the specific structure in the Rectorite.

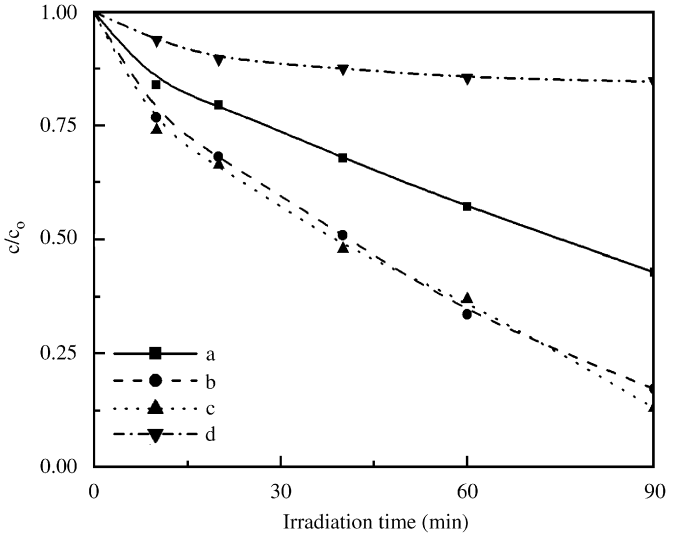

Fig. 7. Photocatalytic activities of the obtained samples: (a) CR0, (b) CR2, (c) CR4, and (d) 3.8 mg CdS derived from hydrothermal process.

The experimental results on photostability for CR0, pure CdS (3.8 mg), and CR4 are summarized in Table 2. Undergoing 5 times repeated photocatalytic experiments, the photodegradation efficiency of the CR4 nanocomposite reduces from 85% to 71%; but the photodegradation efficiency decreases significantly from 15% to 6% for 3.8 mg pure CdS. Those results show that the photostability of the nanocomposite is much better than the pure CdS. The host layers effectively suppress the S^{2-}-oxidization, consequently, retarded the photocorrosion of the CdS in the complex. For further confirmation the photostability of the CdS/Rectorite nanocomposites, Cd^{2+} concentrations in the suspension after photodegradation reaction with 6 h were measured by inductively coupled plasma atomic emission spectrometry (ICP-AES, Beijing Broadcast Instrument Factory, Beijing, China). Using CR1, CR2, CR3, CR4 and CdS as photocatalysts, the results show that Cd^{2+} concentrations in the photocatalytic degradation RB suspension are 0, 0.22, 0.64, 2.03 and 50.3 μg/ml, respectively. Namely, the photocorrosion percent is 0%, 0.005%, 0.010%, 0.024% and 85.02%. It can be seen that pure CdS is easy to be photochemically corroded, whereas this photochemical corrosion on CdS can be markedly restrained by Rectorite hosts. Compared with our previous nanocomposites reported in [34], the present composites show more effective CdS loading and better photoactivity and photostability. Therefore, we can conclude that the

Table 2
The experimental results of photostability for the obtained samples

Repeat times	1	2	3	4	5
CR4 (%)	85	77	74	73	71
CdS (%)	15	13	10	7	6
CR0 (%)	57	35	30	19	13

present materials are more potential in environmental cleanup as a novel purificatory eco-material.

4. Conclusion

The CdS/Rectorite nanocomposites were prepared via hydrothermal methods. The experimental results indicate that the CdS existed in at least three forms: adsorbed at surface, pillared in montmorillonite-like layers of Rectorite and pillared in the new layered structure formed during the hydrothermal process. The CdS nanoparticles in the composites adopt a hexagonal symmetry. The photocatalytic experiments results show that the nanocomposites have much higher photoactivity on the photodegradation of RB than that of the Rectorite and the pure CdS due to the surface adsorptive property, the cooperation or synergetic action of the CdS and the specific structure in the Rectorite. And the nanocomposites have higher stabilities than the pure CdS. The CdS/Rectorite nanocomposite is expected to be useful in various applications, for instance, adsorption and photodegradation of various organic contaminants, this kind of nanocomposite is potential in energy renewal, energy storage and environmental cleanup as a novel purificatory eco-material.

Acknowledgments

This work is supported by the Natural Science Fund of China (20573078), National "863" Foundation (2006AA03Z344), Talented Young Scientist Foundation (2006ABB003) of Hubei Province, China. Dr. T.Y. Peng is indebted to Dr. J.B. Wang, Center of Electron Microscopy, Wuhan University, who has kindly offered the help in HRTEM observation.

References

[1] C.B. Molina, J.A. Casas, J.A. Zazo, J.J. Rodríguez, Chem. Eng. J. 118 (2006) 29–35.
[2] P. Das, I. Kuźniarska-Biernacka, A.R. Silva, A.P. Carvalho, J. Pires, J. Mol. Catal. A-Chem. 248 (2006) 135–143.
[3] J. Carriazo, E. Guélou, J. Barrault, J.M. Tatibouët, R. Molina, S. Moreno, Catal. Today 107–108 (2005) 126–132.
[4] N. Maes, E.F. Vansant, Microporous Mater. 4 (1995) 43–51.
[5] F. Kooli, W. Jones, J. Mater. Chem. 8 (1998) 2119–2124.
[6] F. Kooli, J. Bovey, W. Jones, J. Mater. Chem. 7 (1997) 153–158.
[7] M.A. Maireles-Torres, P. Olivera-Pastor, E. Rodriguez-Castellon, A. Jimenez-Lopez, L. Alagna, A.A.G. Tomlinson, J. Mater. Chem. 1 (1991) 319–323.
[8] S. Yoda, Y. Sakurai, A. Endo, T. Miyata, H. Yanagishita, K. Otake, T. Tsuchiya, J. Mater. Chem. 14 (2004) 2763–2767.
[9] J.L. Valverde, A. de Lucas, F. Dorado, A. Romero, P.B. Garcia, Ind. Eng. Chem. Res. 44 (2005) 2955–2965.
[10] F. Kooli, W. Jones, Chem. Mater. 9 (1997) 2913–2920.
[11] M. Pichowicz, R. Mokaya, Chem. Mater. 16 (2004) 263–269.
[12] F. Figueras, Catal. Rev. Sci. Eng. 30 (1998) 457–462.
[13] D.E.W. Vaughan, ACS Symp. Ser. 368 (1988) 308–313.
[14] R.E. Grim, Clay Minerology, second ed, McGraw-Hill, New York, 1968, pp. 79–83.
[15] J.P. Olivier, M.L. Occelli, Microporous Mesoporous Mater. 57 (2003) 291–296.
[16] M.L. Occelli, A. Bertrand, S.A.C. Gould, J.M. Dominguez, Microporous Mesoporous Mater. 34 (2000) 195–206.
[17] S. Thomas, M.L. Occelli, Clay Clay Miner. 48 (2000) 2–8.
[18] M.L. Occelli, S.A.C. Gould, J. Catal. 198 (2001) 41–46.
[19] M.L. Occelli, J.M. Dominguez, H.J. Eckert, Catal 141 (1993) 510–523.
[20] K. Ohtsuka, Chem. Mater. 9 (1997) 2039–2050.
[21] R.E. Schwerzel, K.B. Spahr, J.P. Kurmer, V.E. Wood, J.A. Jenkins, J. Phys. Chem. A 102 (1998) 5622–5626.
[22] S. Sapra, J. Nanda, D.D. Sarma, F. Abed El-Al, G. Hodes, Chem. Commun. (2001) 2188–2189.
[23] M.K. Arora, A.S.K. Sinha, S.N. Upadhyay, Ind. Eng. Chem. Res. 37 (1998) 3950–3955.
[24] T. Sato, K. Masaki, K. Sato, Y. Fujishiro, A. Okuwaki, J. Chem. Technol. Biotechnol. 67 (1996) 339–344.
[25] (a) W.F. Shangguan, A. Yoshida, Sol. Energy Mater. Sol. C 69 (2001) 189–192;
(b) W.F. Shangguan, A. Yoshida, J. Phys. Chem. B 106 (2002) 12227–12230.
[26] T. Sato, K. Sato, Y. Fujishiro, T. Yoshioka, A. Okuwaki, J. Chem. Technol. Biotechnol. 67 (1996) 345–350.
[27] Z.H. Han, H.Y. Zhu, S.R. Bulcock, S.P. Ringer, J. Phys. Chem. B 109 (2005) 2673–2678.
[28] C. Ooka, S. Akita, Y. Ohashi, T. Horiuchi, K. Suzuki, S. Komai, H. Yoshida, T. Hattori, J. Mater. Chem. 9 (1999) 2943–2952.
[29] M.L. Occelli, A. Auroux, J.G. Ray, Microporous Mesoporous Mater. 39 (2000) 43–56.
[30] M.L. Occelli, Scientific basis for the preparation of heterogeneous catalysts, in: Proceedings of the Fifth International Symposium, Elsevier, Amsterdam, 1991, p. 287.
[31] I. Dekany, L. Turi, G. Galbacs, J.H. Fendler, J. Colloid Interface Sci. 213 (1999) 584–591.
[32] I. Dekany, L. Turi, Z. Kiraly, Appl. Clay Sci. 15 (1999) 221–239.
[33] Y. Fujishiro, S. Uchida, T. Sato, J. Inorg. Mater. 1 (1999) 67–72.
[34] J.R. Xiao, T.Y. Peng, D.N. Ke, L. Zan, Z.H. Peng, Phys. Chem. Minerals 34 (2007) 275–285.
[35] H.L. Hong, L.Y. Tie, Q.L. Bian, Y. Zhou, J. Chin. Electron Microsc. Soc. 24 (2005) 124–129 (in Chinese).
[36] Y. Xie, G.K. Zhang, C.S. Zhu, J. Yu, Ind. Safety Environ. Protect. 30 (2004) 28–32 (in Chinese).
[37] Q. Lu, Z.D. Tang, X.R. Lei, H.F. Liu, Y. Liu, Acta Mineral. Sin. 21 (2001) 27–33 (In Chinese).
[38] H. Weller, H.M. Schmit, U. Koch, A. Foitik, S. Baral, A. Henglein, W. Kunath, K. Weiss, E. Diekmann, Chem. Phys. Lett. 41 (1990) 477–479.